Nuclear Receptor Research
vol. 4 (2017), Article ID 101302, 21 pages
doi:10.11131/2017/101302

AgiAl Publishing House
http://www.agialpress.com/

Research Article

Mutations in Liver X Receptor Alpha that Impair Dimerization and Ligand Dependent Transactivation

Shimpi Bedi, Heather A. Hostetler, and Stanley Dean Rider, Jr.

Department of Biochemistry & Molecular Biology, Boonshoft School of Medicine, Wright State University, 3640 Colonel Glenn Hwy, Dayton, OH 45435, USA

Abstract. Liver X receptor alpha (LXRα) is crucial for the maintenance of lipid and cholesterol homeostasis. Ligand binding and dimerization with retinoid X receptor (RXR) or peroxisome proliferator-activated receptor (PPAR) is required for forming active DNA binding complexes leading to gene regulation. Structure based prediction and solvent accessibility of LXRα LBD shows that residues H383, E387, H390, L414, and R415 which are located in helices 9 and 10 may be critical for mediating protein-protein interactions. In this study, LXRα interface residues were individually mutated to determine their effects on ligand binding, protein-protein association, subcellular localization, and transactivation activity. LXRα L414R and R415A lacked binding to T-0901317, but retained binding to 25-Hydroxycholesterol. *In vitro* assay and a cell based assay demonstrated that LXRα L414R was specifically impaired for interactions with RXRα but not PPARα suggesting that charge reversal at the interface provides selectivity to LXRα dimerization. Furthermore, binding of LXRα L414R or R415A with PPARα exhibited minimal conformational changes in the dimer secondary structure. Interestingly, all LXRα mutants exhibited lower levels of ligand dependent luciferase activity driven by the SREBP-1c or ApoA1 promoter. Taken together, our data demonstrates that intact hydrophobic interactions and salt bridges at the interface mediate efficient ligand-dependent transactivation activities.

Keywords: Liver X receptor alpha, peroxisome proliferator-activated receptor alpha, retinoid X receptor alpha, Sterol Regulatory Element Binding Protein-1c, Apolipoprotein A119.

Corresponding Author
Stanley Dean Rider, Jr.
s.dean.rider@wright.edu

Editor
Enrique Saez

Dates
Received 8 June 2017
Accepted 10 August 2017

1. Introduction

Nuclear hormone receptors PPARα and LXRα are ligand activated transcription factors that are activated by fatty acids and oxysterols respectively [1, 2]. These receptors act as sensors of elevated levels of fatty acids and cholesterol derivatives *via* the receptor ligand binding domain (LBD) to regulate the expression of genes involved in controlling cholesterol and lipid metabolism [3, 4]. PPARα and LXRα can heterodimerize with each other and individually with retinoid X receptor (RXR) with high affinities and the corresponding dimers are the functionally active forms of these receptors [5]. Due to the crucial roles of these receptors in maintaining constant level of lipids in cells, PPARα and LXRα represent interesting targets for the development of pharmacological compounds in the treatment of metabolic disorders [6]. Drugs targeting these receptors exhibit anti-atherogenic, anti-inflammatory, and anti-diabetic effects. These effects, however, are also associated with elevated levels of plasma triglycerides due to upregulation of master lipogenic enzyme SREBP-1c [7, 8]. Thus, there is an immense interest

in investigating regulation of the PPARα-LXRα heterodimer to explore an alternative strategy for the pharmacological manipulation of PPARα and LXRα.

Both nuclear receptors have two well-structured domains, a central DNA binding domain and a C-terminal LBD [9]. In addition to mediating receptor dimerization, the LBD performs a number of functions such as ligand binding, recruitment of coactivators, transcriptional activation, and repression [9–12]. Inspection of the crystal structure of LXRα-RXRβ LBDs (PDB entry 1UHL;Uniport Q13133-1) shows that the LXRα LBD interface is made up of amino acid residues in helices 9 and 10 [13]. Residues lining these helices provide the locus for the majority of heterodimerization and homodimerization interactions. In particular, amino acid residues H383, E387, and H390 (helix9) [13] and L414 and R415 (helix10) are located on the surface of LXRα and a majority of the residues undergo significant changes in accessible surface area upon receptor dimerization. Critical determinants of LXRα dimerization have not been characterized yet and variants of LXRα that exhibit selective dimerization or ligand binding properties are unknown.

Previous work suggests that mutations have the ability to confer selectivity in protein binding. RXRα mutants (A416D, R421L, and A416K) exhibit selectivity in binding with thyroid hormone receptors and retinoid acid receptors [14] Although similar studies in the LBD of LXRα have not been conducted, mutation at R415 to A was found to lack ligand dependent transactivation activity in the context of the ADH promoter when challenged with T0901317 [15]. This suggests that residue R415 may stabilize LXRα-RXR complexes, thus it is likely that loss of interactions between R415 and corresponding residues on RXR would abolish or disorganize dimerization. In addition to causing perturbations in the dimer formation, LXRα mutation R415A may have long-range structural and functional consequences. Consistent with this observation, we hypothesize that charge reversal of key residues at LXRα interface may provide selectivity in the choice of heterodimer binding and hence downstream gene regulation. To test our hypothesis and to investigate the effects of mutating interface residues on LXRα function, individually amino acid residues were mutated at putative protein-protein contact points of LXRα and the effects on dimerization, ligand binding, and transactivation activity were measured.

Single point mutations in the LXRα LBD were generated using site-directed mutagenesis and apparent dissociation constants (K_d) of PPARα-LXRα interactions of mutant proteins relative to wild-type were measured. Circular dichroism (CD) was applied to study (a) the effect of mutations alone on LXRα secondary structure, and (b) the conformational changes induced in the dimers due to protein-protein binding. Bimolecular complementation assays demonstrated that LXRα mutant, L414R, is selectively impaired in dimerization with RXRα but not with PPARα. A previously identified LXRα mutant, R415A, exhibited intact dimerization but showed selective loss in ligand binding to T0901317. Molecular modeling was performed to visualize the orientation of ligands in the LXRα ligand binding pocket and it showed differences between the positioning of ligands between wild-type and mutant receptors consistent with the previous results. Finally, a cell based transactivation assay showed that LXRα L414R lacked transactivation activity when tested in the context of SREBP-1c promoter. On the other hand, LXRα R415A behaved similar to wild-type LXRα in transactivation activity in the context of SREBP-1c promoter, but exhibited lower activity on ApoA1 promoter.

2. Materials and Methods

2.1. Chemicals

All ligands were purchased from Sigma-Aldrich (St. Louis, MO). Cy^{TM}3 Ab labelling kit was purchased from GE Healthcare. BiFC cloning vectors pBiFC-VN173 (pFLAG-Venus 1-172), pBiFC-CN173 (pFLAG-Venus 1-172), and pBiFC-CC155 (pHA-ECFP 155-238) were supplied by Dr. Chang-Deng Hu (Purdue University).

2.2. Mutagenesis and purification of recombinant mutant hLXRα proteins

The LXRα protein sequence in our investigation is based on isoform 1 (Uniport accession Q13133-1). The purification of recombinant wild-type 6xHis-GST-hLXRα and 6xHis-GST-hPPARα proteins have been described [16]. LXRα mutant proteins were generated through overlap PCR of 6xHis-GST-hLXRα using the following primers:

LXR H383E	Forward 5'- AGAGGCTGCAGGAGACATATGTGGA -3'
	Reverse 5'- TCCACATATGTCTCCTGCAGCCTCT -3'
LXR E387Q	Forward 5'- CACACATATGTGCAAGCCCTGCAT -3'
	Reverse 5'- ATGCAGGGCTTGCACATATGTGTG
LXR H390E	Forward 5'- GAAGCCCTGGAAGCCTACGTC -3'
	Reverse 5'- GACGTAGGCTTCCAGGGCTTC -3'
LXR L414R	Forward 5'-CTGGTGAGCCGCCGGACCCTG-3'
	Reverse 5'-CAGGGTCCGGCGGCTCACCAG-3'
LXR R415A	Forward 5'-CTGGTGAGCCTCGCGACCCTG-3'
	Reverse 5'-CAGGGTCGCGAGGCTCACCAG-3'

The PCR products containing *EcoRI-HF* and *NotI-HF* sites were used to replace wild-type LXRα with the mutant LXRα PCR fragment in the appropriate vectors. The presence of single point mutations was confirmed by DNA sequencing. Plasmids were then transformed into Rosetta 2 competent cells and used to produce recombinant mutant full-length hLXRα proteins through affinity chromatography as described for hPPARα and wild-type hLXRα [16–18]. Protein concentration was determined by the Bradford assay (Bio-Rad, Hercules, CA) and by absorbance spectroscopy using the molar extinction for the protein. Protein purity was determined by sodium dodecyl sulfate-polyacrylamide gel electrophoresis (SDS-PAGE), followed by Coomassie Blue staining.

2.3. Quenching of endogenous fluorescence of mutant LXRα by Ligands

The direct binding of LXRα mutant recombinant proteins to non-fluorescent ligand T-0901317 was determined by quenching of intrinsic LXRα aromatic amino acid fluorescence. Briefly, mutant LXRα (0.1 μM) was titrated with increasing concentrations of T-0901317 in PBS, pH7.4. Emission spectra from 300-400 nm were obtained at 24°C upon excitation at 280 nm with a

PC1 photon counting spectrofluorometer (ISS Inc., Champaign, IL). Data were corrected for background and inner filter effects, and maximal intensities were used to calculate the apparent dissociation constant (K_d) values as described [17, 18].

2.4. Circular dichroism spectroscopy

Circular dichroism was used to examine changes in the secondary structure upon heterodimerization of hPPARα with each of the mutant hLXRα proteins. Briefly, CD spectra of protein complexes were obtained by use of a Jasco J-815 CD spectrometer. Circular dichroic spectra of a mixture of PPARα and wild-type or mutant LXRα (0.2 μM final concentration each in 30 mM NaCl, 2 mM Tris, pH 8.0, 0.04% glycerol buffer) were measured in the presence and absence of ligands. Spectra was recorded from 260 to 187 nm with a bandwidth of 2.0 nm, sensitivity of 10 millidegrees, scan rate of 50 nm/min and a time constant of 1 s. Ten scans were averaged for percent compositions of α-helices, β-strands, turns and unordered structures with the CONTIN program of the CDpro software package [16–19]. The CD spectrum of the mixed proteins was compared to a theoretical spectrum of combined but noninteracting proteins. The theoretical spectrum was calculated by averaging the spectra of each protein in the mixture analyzed separately at a concentration equal to that in the mixture as described [16].

2.5. Protein-protein binding experiments

Recombinant PPARα was fluorescently labeled with Cy3 dye using Fluorolink-antibody Cy3 labeling kit (Amersham Biosciences, Pittsburgh, PA) as described [16].Emission spectra (560-650 nm) of 25 nM Cy3-labeled PPARα were recorded in PBS, pH 7.4 upon excitation at 550 nm with increasing concentrations of unlabeled LXRα in a Cary Eclipse fluorescence spectrophotometer at 24^0C. The spectra were corrected for background (buffer, solvent, and protein alone), and the maximal intensities were recorded. To determine the effects of ligands on LXRα-PPARα interaction, the experiments were repeated in the presence of each ligand at a concentration determined by their binding affinities. Protein-protein binding curves were analyzed by nonlinear regression analysis using the ligand binding function in Sigma Plot (SPSS Inc., Chicago, IL). The apparent dissociation constant (K_d) values were obtained as previously described [16].

2.6. Bimolecular fluorescence complementation assay for visualization of dimers in living cells

Plasmids encoding full-length 6xHis-GST hPPARα, 6xHis-GST hLXRα, and 6xHis-GST hRXRα were digested with *BamH1-HF/Not1-HF* or *EcoR1/Not1* and ligated into pBiFC vectors to generate Venus-hPPARα, ECFP-hLXRα, and Cerulean-hRXRα plasmids. All constructs were verified by DNA sequencing. COS-7 cells were grown to 50–70% confluence in DMEM supplemented with 10% FBS at 37˚C with 5% CO_2 in a humidified chamber. Cells were seeded onto Lab-Tek chambered cover glass and transfected with 0.7 μg of each BiFC plasmid using Lipofectamine 2000. The growth media and transfection reagent were replaced with serum-free media twenty-four hours after transfection and allowed to grow for additional 20-24 hours before image acquisition using a fluorescence microscope [20].

2.7. Molecular docking

The LBD of LXRα was extracted from the crystal structure of LXRα-RXRβ (PDB entry 1UHL) using Swiss PDB Viewer (spdbv) [13]. The mutant LXRα files utilized as input for docking were prepared using AutoDock Tools and subjected to energy minimization. Docking of T-0901317 to the LXRα LBD was performed using AutoDock Vina 1.1.2 and FlexiDock^{TM} module on SYBYL-X 2.0 as described [18]. The output obtained from AutoDock vina was used to guide prepositioning of the ligand in the ligand binding domain of LXRα. In addition to ligands, rotatable bonds of side chains of binding site residues were allowed to move during the docking procedure. The output generated consisted of docking poses and binding energies that were ranked in the order of the most favorable to the least favorable binding energy. The most energetically favorable conformations were chosen for further analysis as described [18].

2.8. Mammalian expression plasmids

Thegeneration ofpSG5-hPPARα and pSG5-hLXRα plasmids has been described [16]. Mutant hLXRα mammalian expression plasmids were generated by subcloning *MSCI-XhoI* hLXRα mutant fragment from 6xHis-GST hLXRα into *MSCI-XhoI* site of pSG5-hLXRα. The human sterol regulatory element binding protein 1c (hSREBP-1c) minimal promoter (−520 to −310) [8] containing the LXREwas cloned into the pGEM-T easy vector (Promega) and subsequently transferred into *Kpn*I-*Xho*I sites of pGL4.17 (Promega) to produce hSREBP-1c-pGL4.17. The human ApoA1 promoter was amplified with the following primers: tggtaccAGAGGTCTC-CCAGGCTAAGG and cgaattcGCAGTAACCTCTGCCTCCTG. The PCR product was cloned into the pGEM-T easy vector and subsequently transferred into pGL4.17 to produce hApoA1-pGL4.17. All constructs were verified by DNA sequencing.

2.9. Cell culture and transactivation assay

COS-7 cells (ATCC, Manassas, VA) were grown in DMEM supplemented with 10% fetal bovine serum (Invitrogen, Grand Island, NY) at 37˚C with 5% CO2 in a humidified chamber. Cells were seeded onto 24-well culture plates and transfected with 0.4 μg of each full- length mammalian expression vector (pSG5-hPPARα, pSG5- wild-type or mutant hLXRα or pSG5-hRXRα) or empty plasmid (pSG5), 0.4 μg of the LXRE LUC reporter construct (hSREBP-1c) or hApoA1, and 0.04 μg of the internal transfection control plasmid pRL-CMV (Promega Corp., Madison, WI) with Lipofectamine^{TM} 2000 (Invitrogen, Grand Island, NY). Following transfection incubation, medium was replaced with serum-free medium for 2 h, ligands (10 μM) were added, and the cells were grown for an additional 20 h. Firefly luciferase activity, normalized to *Renilla* luciferase (for transfection efficiency), was determined with the dual luciferase reporter assays system (Promega, Madison, WI) and measured with a SAFIRE2 microtiter plate reader (Tecan Systems, Inc. San Jose, CA). The sample with no ligand was arbitrarily set to 1 [16].

Table 1: Exposure of Amino Acid Residues Predicted at LXRα Interface predicted using InterProSurf Protein-Protein Interaction Server (http://curie.utmb.edu/prosurf.html). Crystal structure of the protein complex of LXRα-RXRβ (PDB 1UHL) was analyzed to predict potential interface regions on the surface of LXRα protein using the probe radius of 1.4 A˚.

Amino Acid Residue	Residue Number	Monomer Area	Complex Area	Change in Accessible Surface Area
H	383	106	67	39
E	387	79	15	64
H	390	83	39	44
R	415	93	17	76

2.10. Statistical analysis

Data were analyzed by Sigma Plot^{TM} (Systat Software, San Jose, CA) and a one-way ANOVA was used to evaluate overall significance. The results are presented as mean ± SEM. The confidence limit of $p < 0.05$ was considered statistically significant.

3. Results

3.1. Generation of LXRα mutants

To identify putative residues at the LXRα interface that may mediate interactions with PPARα, we generated site specific mutants of LXRα based on solvent accessibility of residues located in helices 9 and 10. These helices form the LXRα interface in the three dimensional crystal structure of LXRα-RXRβ crystal structure [PDB 1UHL,13]. As shown in Figure 1A, amino acid residues H383, E387, H390, L414, and R415 are located on the surface of helices 9 and a majority of these residues undergo significant changes in solvent accessibility upon dimerization (Table 1). These residues were predicted to stabilize the LXRα interface. With the intent of neutralizing charge at the interface to generate LXRα mutants that may have altered receptor selectivity, H to E, E to Q, and L to R, LXRα mutants were generated. The assignment of helices H9 and H10 together with the point mutations of amino acids implicated in receptor dimerization are shown in Figure 1B.

3.2. Full-length mutant LXRα protein purification

Recombinant full-length mutant hLXRα proteins were expressed in Rosetta 2 cells and purified using affinity chromatography as described for wild-type LXRα protein [16]. SDS-PAGE and Coomassie blue staining indicated predominant bands of 50 kDa corresponding to the expected size of full-length hLXRα, for which purity was determined to be approximately 75% purity (Figure 2). The single point mutations of LXRα did not dramatically alter the secondary structure as was evident using far-UV CD spectrometry (data not shown).

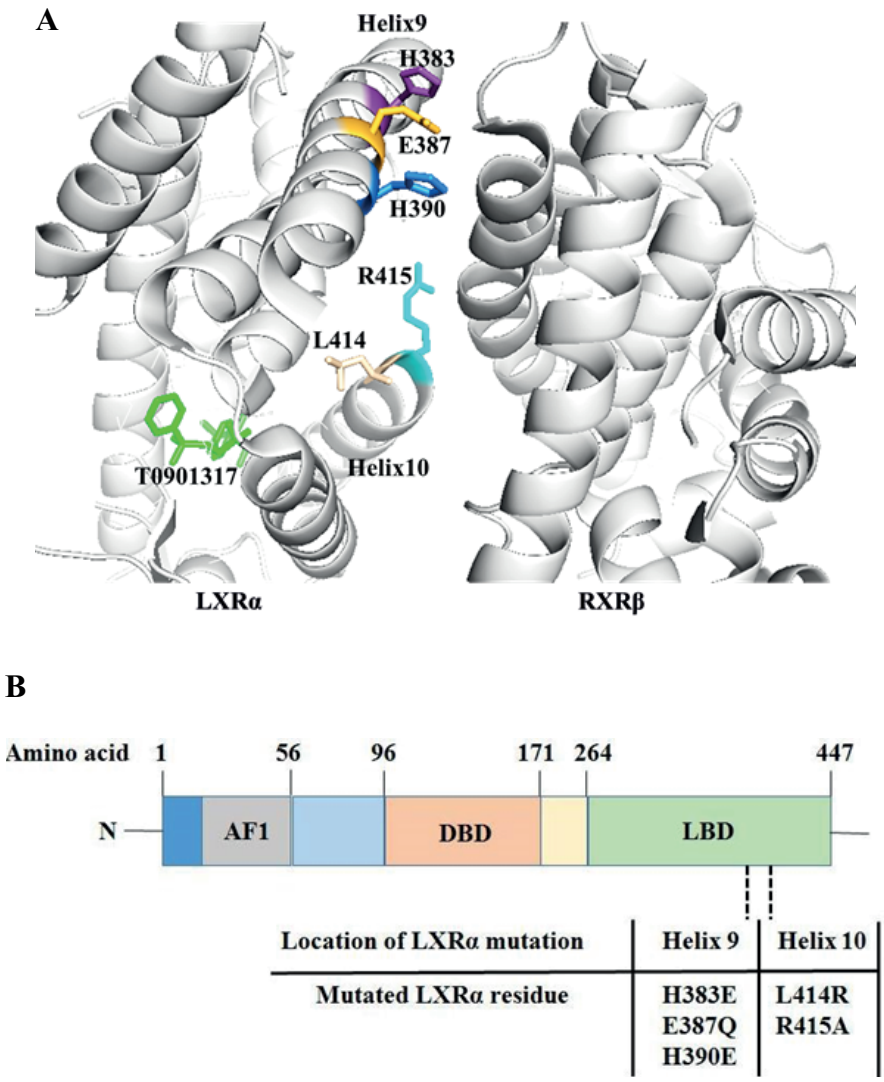

Figure 1: Interface of LXRα-RXRβ heterodimer showing the positioning of solvent accessible residues (A) Contacts across the LXRα dimer interface. Location of amino acid residues H383, E387, H390, L414, and R415 in helices 9 and 10 across the LXRα-RXRβ heterodimer as proposed in the crystallographic structure (PDB 1UHL) (B) Schematic representation of the LXRα domain structure showing single point mutations. All numbering is based on LXRα isoform 1 (Uniport Q13133-1).

3.3. Ligand binding profile of LXRα mutants

The effect of each LXRα mutation on ligand binding was investigated. Apparent dissociation constant (K_d) values of purified recombinant proteins for T-0901317 were determined using intrinsic quenching of LXRα aromatic amino acids. As seen in Figure 3, titration of wild-type and H383E LXRα proteins with T-0901317 yielded sharp saturation curves with maximal changes in fluorescence at low protein concentrations suggesting high affinity binding (apparent $K_d = 4 \pm 1$ nM and 4 ± 2 nM respectively). Titration of LXRα E387Q and H390E proteins with T0901317 also yielded decrease in the fluorescence of proteins, however, the slopes of the binding curves were shallower compared to wild-type and H383E LXRα suggesting lower affinity ligand binding (apparent $K_d = 29 \pm 8$ nM and 34 ± 8 nM respectively). Interestingly, T0901317 did not cause significant changes in the intrinsic fluorescence of the L414R and R415A proteins

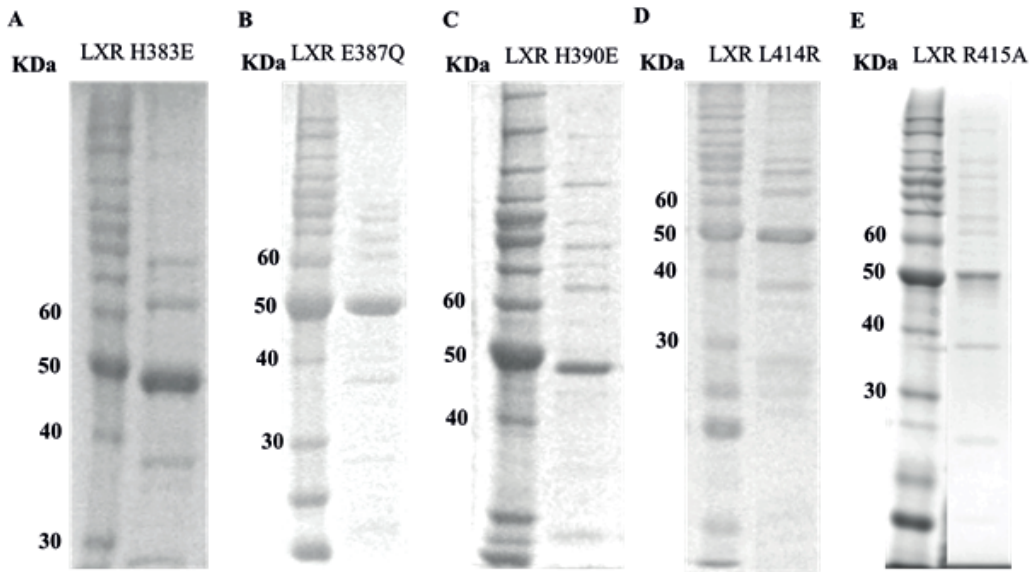

Figure 2: SDS-PAGE and Coomassie blue staining of purified recombinant hLXRα mutant proteins (A) H383E, (B) E387Q, (C) H390E, (D) L414R, and (E) R415A. The prominent bands at approximately 50KDa are full-length, untagged recombinant mutant LXRα proteins.

suggesting no binding. All mutants, except H390E, bound the endogenous ligand 25-HC at nanomolar concentrations similar to that for wild-type LXRα suggesting that mutations did not have detrimental effects on LXRα binding to the relatively weaker endogenous ligand 25-HC (Appendix Figure 1 available online at `http://www.agialpress.com/journals/nurr/2017/101302/`). None of the mutations compromised the folding of the protein as determined by the circular dichroic spectra of the individual proteins (data not shown). The selectivity in ligand binding was further investigated through computational-based molecular modeling of T-0901317 to energy-minimized wild-type, L414R, and R415A LXRα LBDs (Figure 3G). The deviation from the positioning of ligand in wild-type was greater in the R415A mutant than in the L414R LXRα mutant. Calculation of the corresponding hydrogen bonds and hydrophobic interactions between the ligand and residues lining the LXRα LBP was performed using LIGPLOT analysis. The head group of T-0901317 formed hydrogen bonds with His421 in wild-type, H383E, E387Q, and H390E, but not with L414R and R415A LXRα (Appendix Figure 2 available online at `http://www.agialpress.com/journals/nurr/2017/101302/`).

3.4. Computational-based prediction of ligand binding in LXRα mutants

In silico molecular docking allows distinction of binding molecules from nonbinding molecules and is a method of choice for identification of potential binding sites for ligand-receptor complexes. Docking was employed to evaluate and compare ligand binding scores of LXRα protein upon introducing mutations at the interface (Table 2). As a control, T-0901317 was docked into the LBD of wild-type LXRα that resulted in a ligand conformation identical to that seen in the reported crystal structure (PDB 1UHL). T-0901317 was then docked into the energy minimized LBDs of individual LXRα mutants using the same docking parameters. The binding scores were compared with the experimentally determined affinities of T-0901317 binding to

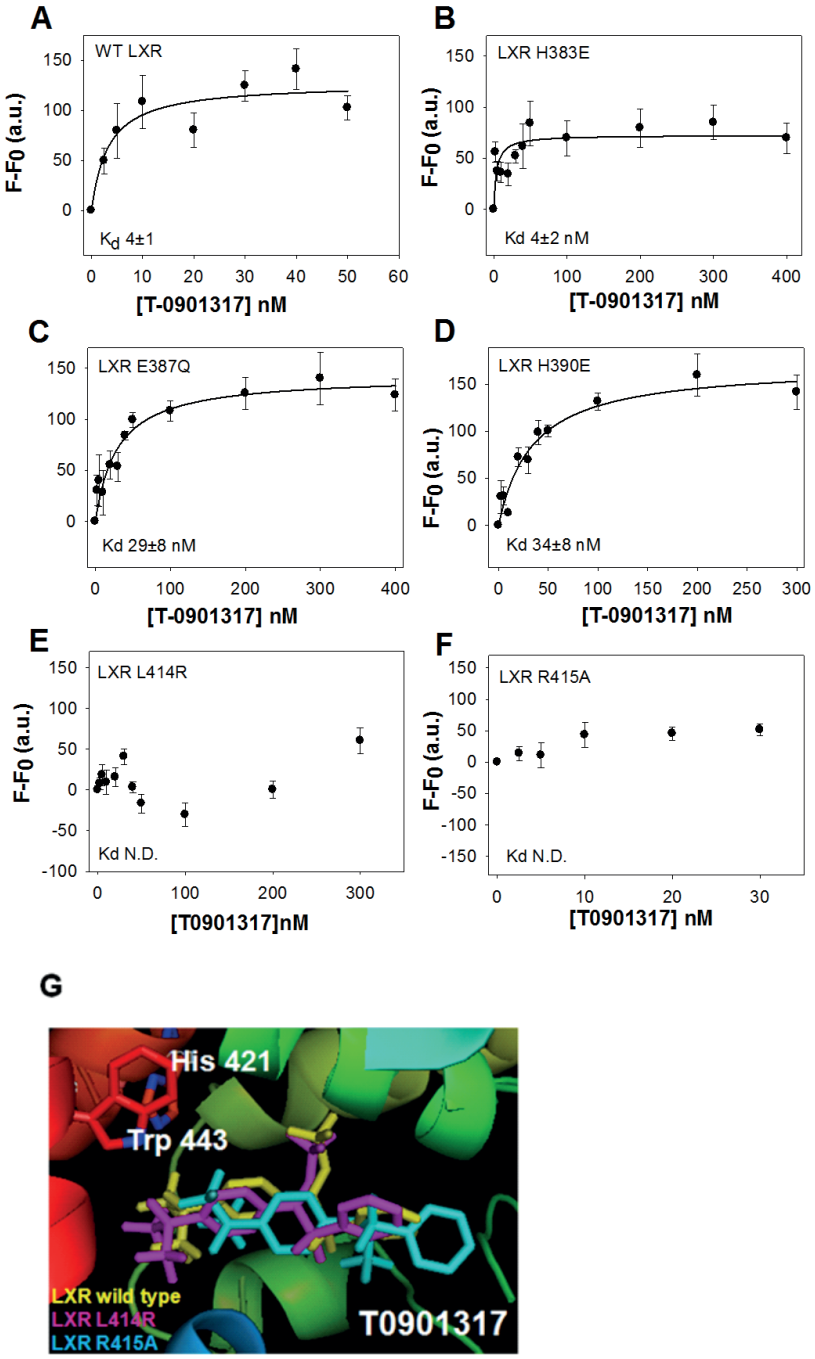

Figure 3: Intrinsic quenching of (A) wild-type, (B) H383E, (C) E387Q, (D) H390E, (E) L414R, and (F) R415A LXRα aromatic amino acids by binding to T-0901317. Three independent experiments were performed for each analysis. (G) Docking of T-0901317 to the LXRα LBD shows the relative positioning of ligand in the ligand binding pocket of the receptor. LXRα LBD was extracted from the crystal structure of LXRα-RXRβ (PDB entry 1UHL).

LXRα. As the apparent K_d values for ligand binding increased in the mutants, the binding scores also increased suggesting a decrease in affinity of T-0901317 for the mutants. One exception was LXRα H383E that bound T-0901317 with a similar affinity as wild-type, but yielded a less favorable binding score from the docking simulation. It is important to consider here that

Table 2: The binding scores of T-0901317 binding to LXRα (Kcal.mol^{-1}) protein-ligand complexes were estimated using the FlexiDock program in SYBYL-X 2.0 (Tripos, St. Louis, MO).

Protein	T-0901317
LXRα wild-type	−2047
LXRα H383E	−1421
LXRα E387Q	−1332
LXRα H390E	−1709
LXRα L414R	−1891
LXRα R415A	−1231

Table 3: Binding affinities of LXRα mutants for PPARα in the absence or presence of ligands.

	Wild-type K_d (nM)	H383E K_d (nM)	E387Q K_d (nM)	H390E K_d (nM)	L414R K_d (nM)	R415A K_d (nM)
No ligand	8 ± 2	7 ± 1	10 ± 2	27 ± 11	13 ± 5	14 ± 3
T0901317	35 ± 6	13 ± 2	53 ± 9	9 ± 1	34 ± 6	23 ± 17
25HC	16 ± 3	2 ± 0.5	49 ± 12	5 ± 1	2 ± 0.7	67 ± 13
C16:0 FA	104 ± 40	7 ± 1	27 ± 11	8 ± 1	2 ± 0.2	39 ± 22

the ranking of the binding scores assigned by the docking simulation is not an indication of binding constants, since binding scores are an approximation which must be considered in the context of ligand orientation. Perturbation observed in ligand binding led us to further hypothesize that compromised ligand binding observed in mutants may be coupled to impaired LXRα dimerization.

3.5. Dimerization of LXRα mutants with PPARα

Fluorescence spectroscopy was used to determine how efficiently each mutated form of LXRα dimerized with PPARα. Purified PPARα protein was fluorescently labeled with Cy3 dye at essentially one dye per protein molecule. Protein-protein binding curves were generated by plotting quenching of Cy3 dye as a function of LXRα concentration as previously described [16]. The binding dissociation constant values (K_d) of each LXRα mutant- PPARα dimer were determined. In the absence of added ligand, the K_d values determined for PPARα binding to the wild-type LXRα and each of the mutants were found to range between 8 and 27 nM concentrations (Table 3). As seen in Figure 4, titration of Cy3-labeled PPARα with increasing concentrations of wild-type LXRα resulted in sharply saturable binding curve at a low protein concentration indicative of high affinity binding. Single amino acid substitutions H383E and E387Q also generated binding curves, with affinities that were comparable to wild-type. Titration of Cy3-PPARα with H390E, L414R, and R415A exhibited weaker quenching of Cy3 fluorescence and weak binding was detected compared to wild-type LXRα. Estimation of the apparent dissociation constants of PPARα binding to LXRα mutants showed K_d values to be H383E < Wild-type < E387Q < L414R<R415A < H390E (Table 3). L414R not only bound PPARα with a weaker affinity, it showed weaker binding to RXRα as well (Appendix Figure 3 available online at `http://www.agialpress.com/journals/nurr/2017/101302/`) suggesting that residue L414 may be critical for protein-protein interactions of LXRα.

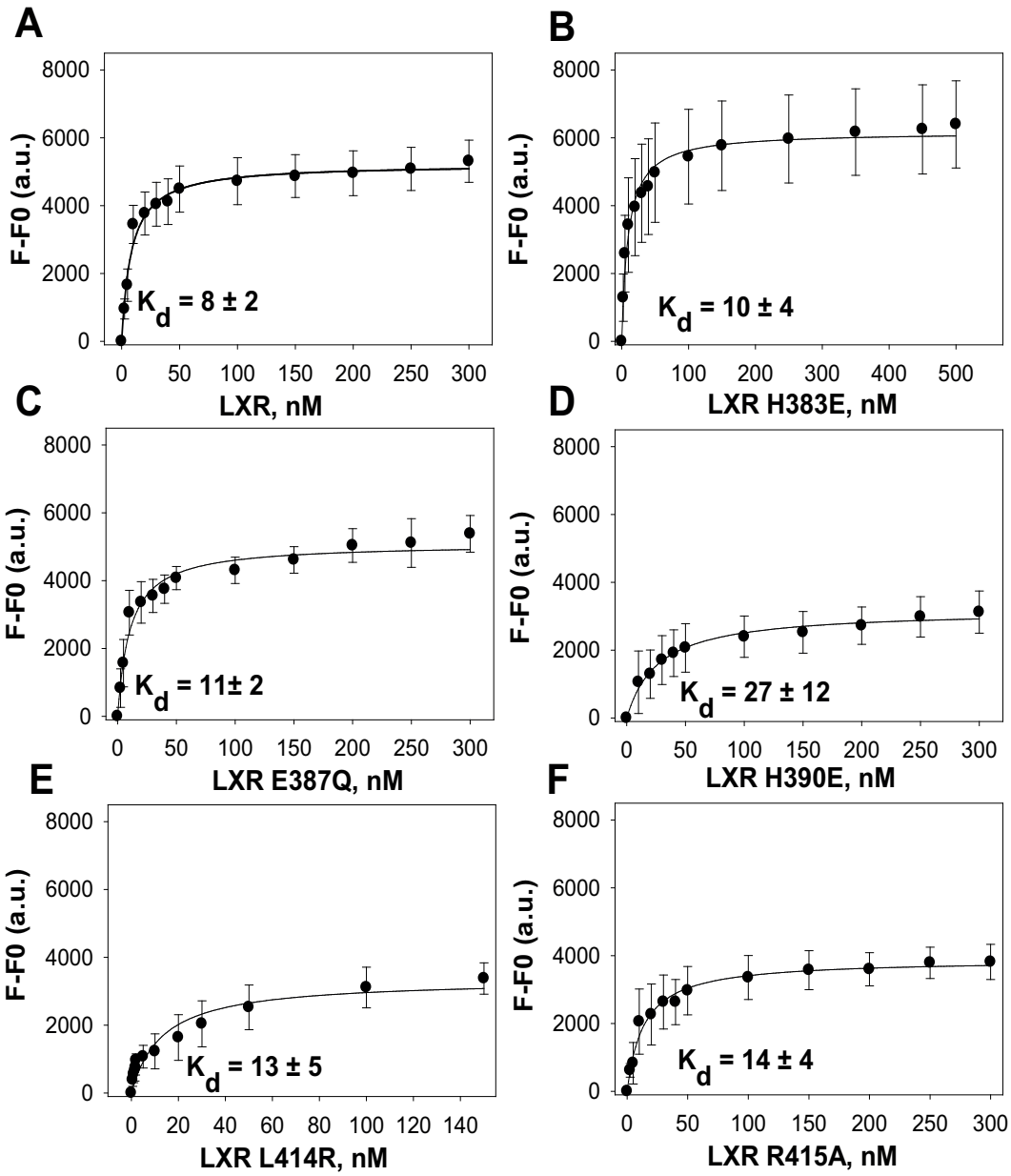

Figure 4: Effects of mutations on dimerization of LXRα with PPARα. Cy3-labeled PPARα was titrated against increasing concentrations of unlabeled LXRα in the absence of ligand. Representative curves from fluorescence binding experiments are shown for binding of each LXRα mutant to PPARα. At least three independent experiments were performed for each analysis. K_d values represent means ± the standard error.

To determine the potency of ligands to affect protein-protein interactions, the binding affinities of PPARα for each LXRα mutant were determined in the presence of ligands as described [16]. The K_d values of each complex upon ligand binding are summarized in Table 3. The binding of T0901317 decreased LXRα-PPARα interactions in wild-type, H383E, E387Q, L414R, and R415A mutants. H390E LXRα bound PPARα with three-fold higher affinity compared to wild-type. The addition of LXRα natural ligand, 25HC, decreased binding of PPARα to wild-type, E387Q, and R415A LXRα and enhanced binding to H383E, H390E, and L414R mutants. The addition of PPARα agonist, palmitic acid, did not affect binding of H383E to PPARα, decreased the interaction of PPARα with wild-type, E387Q, and R415A LXRα, and enhanced

Table 4: Secondary structures of hLXRα and hPPARα proteins in the absence of ligands[a].

Proteins	α-helix regular H(r)%	α-helix distort H(d)%	β-sheet regular S(r)%	β-sheet distort S(d)%	Turns T%	Unordered U%
LXRα	29.7 ± 1.0	23.3 ± 0.8	10.0 ± 1.0	11.0 ± 1.0	14.3 ± 2.0	11.0 ± 2.0
PPARα	28.0 ± 0.0	19.0 ± 1.0	9.3 ± 1.0	8.0 ± 1.0	14.3 ± 0.6	20.3 ± 2.0
PPARα/LXRα (Obs)	32.3 ± 1.2[b]	25.7 ± 0.6[b]	8.3 ± 0.6	8.0 ± 1.0	12.3 ± 0.3	13.0 ± 2.0
PPARα/LXRα (Calc)	27.0 ± 0	22.0 ± 1.0	8.0 ± 0.0	10.0 ± 0.0	15.0 ± 1.0	17.5 ± 1.5
PPARα/LXRα H383E (Obs)	24.0 ± 2.0	16.0 ± 1.0	10.5 ± 0.5[b]	8.0 ± 0.0	17.5 ± 1.5	24.5 ± 0.5[b]
PPARα/LXRα H383E (Calc)	21.5 ± 1.5	17.5 ± 1.5	14.0 ± 0.5	10.5 ± 3.5	17.0 ± 2.0	19.5 ± 0.6
PPARα/LXRα E387Q (Obs)	28.0 ± 0.0[b]	22.3 ± 0.6	8.6 ± 0.3	8.0 ± 1.0[b]	13.7 ± 0.3	19.9 ± 1.5[b]
PPARα/LXRα E387Q (Calc)	23.5 ± 0.5	23.5 ± 0.5	9.5 ± 1.5	14.0 ± 0.0	15.0 ± 1.0	13.5 ± 0.5
PPARα/LXRα H390E (Obs)	31.5 ± 0.5[b]	17.0 ± 1.0	10.0 ± 0.0	9.0 ± 1.0	12.0 ± 2.0	20.5 ± 0.5[b]
PPARα/LXRα H390E (Calc)	25.5 ± 0.9	15.8 ± 0.8	9.5 ± 1.1	8.7 ± 0.7	14.5 ± 0.6	25.2 ± 0.5
PPARα/LXRα L414R (Obs)	26.7 ± 0.8	19.3 ± 0.8	7.6 ± 0.3[b]	6.6 ± 0.3	16.0 ± 0.5	23.3 ± 0.8[b]
PPARα/LXRα L414R (Calc)	27.5 ± 0.5	18.0 ± 0.0	5.5 ± 0.5	6.0 ± 0.0	16.5 ± 0.5	26.0 ± 0.0
PPARα/LXRα R415A (Obs)	29.2 ± 0.8	23.4 ± 0.8	10.8 ± 0.5[b]	8.0 ± 0.6	12.8 ± 0.9	16.4 ± 1.3
PPARα/LXRα R415A(Calc.)	30.5 ± 0.5	23.5 ± 1.5	7.0 ± 1.0	8.5 ± 3.5	13.0 ± 2.0	16.5 ± 4.5

[a]Definitions: Obs, obtained experimentally; calc, calculated average. Significant difference between observed and calc for each protein mixture (n = 4-6). [b]$p < 0.05$.

binding of H390E and L414R to PPARα (Table 3). These observations suggest that complexes composed of PPARα and LXRα mutants respond differentially to the addition of ligands.

3.6. Circular dichroism: conformational changes in dimers composed of LXRα mutants and PPARα

Nuclear receptors are known to undergo conformational changes in the secondary structure upon binding to ligands or other macromolecules. Previous work demonstrated that PPARα and LXRα undergo a conformational change upon interaction [16]. The CD spectra of mutant LXRα proteins alone were qualitatively similar to that of wild-type suggesting that mutations do not impact the overall secondary structure of the mutant proteins (data not shown). To examine protein-protein interactions between PPARα and LXRα mutants, experimentally determined molar ellipticity observed upon mixing of proteins (Obs.) was compared to the average of the sum of the ellipticities of the unmixed proteins (Calc.) using circular dichroism (CD). As seen in Figure 5, spectra of mixtures of each mutant LXRα H383E, E387Q, and H390E with PPARα exhibited a more negative ellipticity at 222 and 208 nm similar to the spectra observed with wild-type LXRα-PPARα mixture. This suggests that binding of wild-type LXRα, and LXR H383E, E387Q, and H390E with PPARα resulted in a slight increase in the overall α-helical content. The observed spectra of LXRα L414R and R415A, in the presence of PPARα, either overlaid the calculated spectra or showed insignificant changes at the wavelengths of 222 and 208 nm. This indicates that binding of PPARα with LXRα L414R and R415A mutants of LXRα

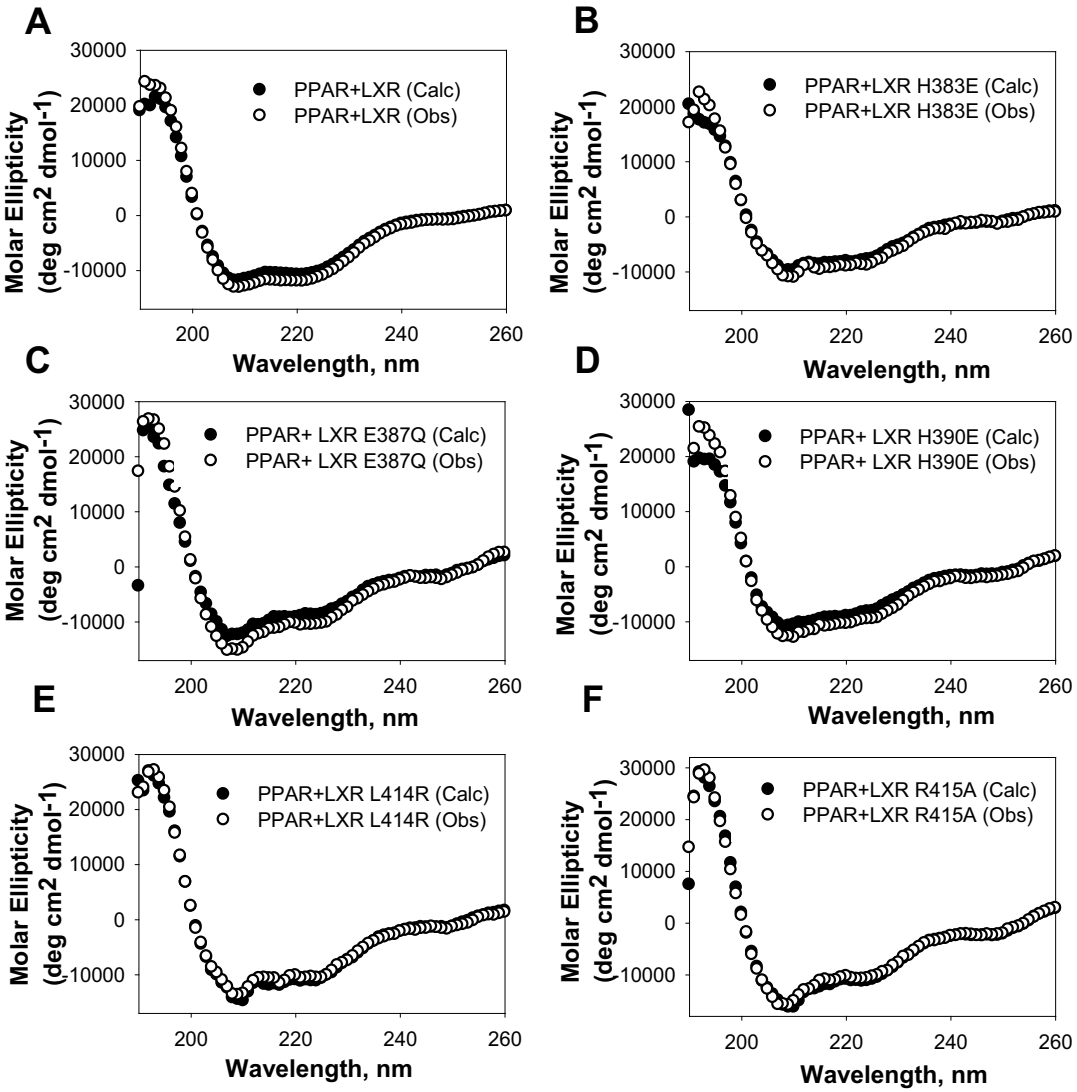

Figure 5: Far UV CD of the mixture of PPARα and LXRα proteins. Experimentally observed (Obs, open circles) circular dichroic spectrum of a mixture of 0.2 μM PPARα and 0.2 μM (A) wild-type, (B) H383E, (C) E387Q, (D) H390E, (E) L414R, and ((F) R415A LXRα compared to the calculated average (Calc, closed circles) of the individually obtained PPARα and LXRα spectra representing non-interacting proteins. The amino acid molarity for each spectrum was 0.0002 M, and each spectrum represents the average of at least three replicates, scanned 5 times per replicate.

is not accompanied by any detectable changes in the overall secondary structures. Quantitative analyses confirmed these data, with no significant changes observed with L414R and R415A ;binding to PPARα (Table 4). Since, the mutants retained binding to either T-0901317 or 25-HC, the effect of ligands on the secondary structure of the dimers composed of PPARα and each of the LXRα mutants was investigated. None of the ligands tested caused significant ligand induced structural changes in dimers composed of PPARα and L414R or R415A (Appendix Figure 4 available online at `http://www.agialpress.com/journals/nurr/2017/101302/`). This suggests that ligands cause structural changes in the individual proteins, but not in the dimer composed of PPARα and LXRα L414R or R415A.

3.7. Analysis of dimers in living cells using bimolecular fluorescence complementation assay (BiFC)

The ability of LXRα mutants to form heterodimers with RXRα and PPARα in living cells using the fluorescence complementation assay was determined. BiFC plasmids encoding ECFP-LXRα, Cerulean-RXRα, and Venus-PPARα were generated for transfection in mammalian cells. COS-7 cells were transiently co-transfected with BiFC plasmids and dimerization was evaluated by fluorescence microscopy. As seen in Figure 6, ECFP LXRα-Cerulean RXRα and ECFP LXRα-Venus PPARα complexes yielded CFP and YFP fluorescent signals respectively in a substantial fraction of cells suggesting that the BiFC system has the sensitivity to detect LXRα-RXRα and LXRα-PPARα interactions. A similar approach was used to investigate the effect of LXRα interface mutations on dimerization. As seen in Figure 6, complexes of LXRα mutants H383E, E387Q, H390E, and R415A with PPARα or RXRα showed nuclear localization and were indistinguishable from wild-type complexes. Co-transfection of mutant L414R with RXRα and PPARα resulted in a robust YFP fluorescence but non-existent levels of CFP fluorescence suggesting that LXRα L414R specifically inhibited LXRα interaction with RXRα but not with PPARα. The LXRα-PPARα BiFC result obtained in cells is consistent with the *in vitro* binding data showing that all LXRα mutants retained their abilities to bind PPARα. A parallel protein-protein binding experiment in solution with RXRα showed that LXRα L414R bound RXRα but with a lower affinity compared to LXRα wild-type or R415A (Supplementary Figure 3 available online at `http://www.agialpress.com/journals/nurr/2017/101302/`). Immunoblot analysis revealed lower expression of RXRα protein levels in samples co-transfected with L414R mutant compared to wild-type and other mutated LXRα plasmids. This suggests that partner receptor that is unable to dimerize with LXRα or binds poorly to PPARα undergoes degradation (Appendix Figure 1 available online at `http://www.agialpress.com/journals/nurr/2017/101302/`).

3.8. Residues at the LXRα interface are required for ligand-dependent transactivation activity

The SREBP-1c promoter contains two LXREs and is activated by LXR overexpression presumable through dimerization with endogenous RXR [22]. No information exists on the identity of genes regulated by LXRα-PPARα heterodimers. However, unpublished data from our laboratory has identified human ApoA1 promoter to contain putative nucleotide sequences that preferentially binds LXRα-PPARα heterodimer. The effects of mutations on the ability of LXRα to dimerize efficiently and hence transactivate a known promoter (SREBP-1c) and a novel promoter (ApoA1) were evaluated using a luciferase reporter assay. Figure 7 illustrates the effects of overexpression of wild-type or mutant LXRα in COS7 cells in the absence or presence of 25HC on SREBP-1c promoter activity.

Since COS7 cells express low levels of endogenous LXRα and PPARα proteins, interference of endogenous protein with the analysis of expressed proteins was unlikely. As shown in Figure 7, wild-type LXRα activation of SREBP-1c promoter was slightly enhanced with the addition of 25-HC. Overexpression of mutants H383E, E387Q, and H390E exhibited an increase in

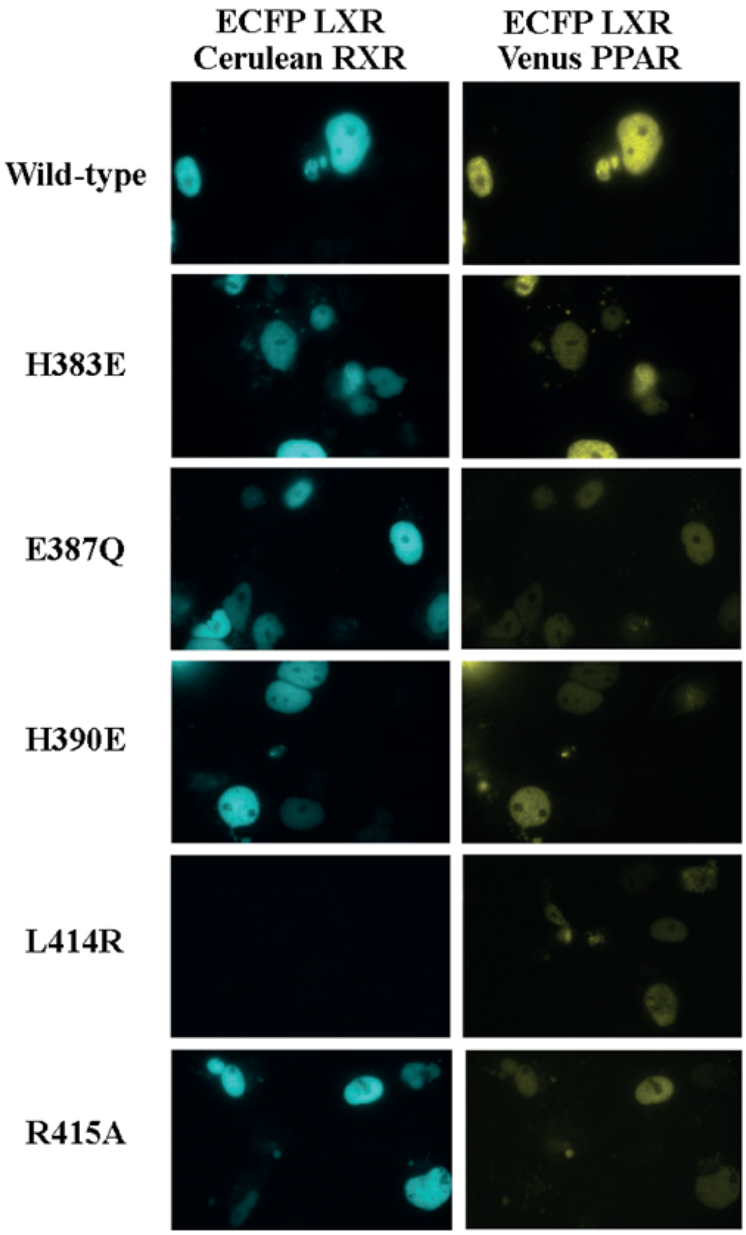

Figure 6: Visualization of protein complexes composed of PPARα and (A) wild-type, (B) H383E, (C) E387Q, (D) H390E, (E) L414R, and (F) R415A LXRα in living cells using Bimolecular Fluorescence Complementation (BiFC) analysis. Fluorescence images of COS-7 cells expressing ECFP-LXR, Venus-PPAR, and Cerulean-RXR proteins were acquired 24 hr after transfection with indicated plasmids.

basal promoter activity, whereas R415A exhibited similar basal activity, and L414R exhibited lower basal activity compared to wild-type LXRα. Interestingly, the basal activities of LXR H383E, E387Q, and H390E were higher than the levels displayed by wild-type LXRα in the presence of 25-HC. This suggests that these mutations resulted in a functional change that was independent of ligand binding for interacting with the SREBP-1c promoter. LXRα activation of the SREBP-1c promoter in transfected COS7 cells was suppressed by cotransfection of PPARα (data not shown) consistent with the findings of Yoshikawa *et al.* [22]. Mutants H383E, E387Q, and H390E exhibited a ligand-induced repression of the promoter activity, whereas, L414R and

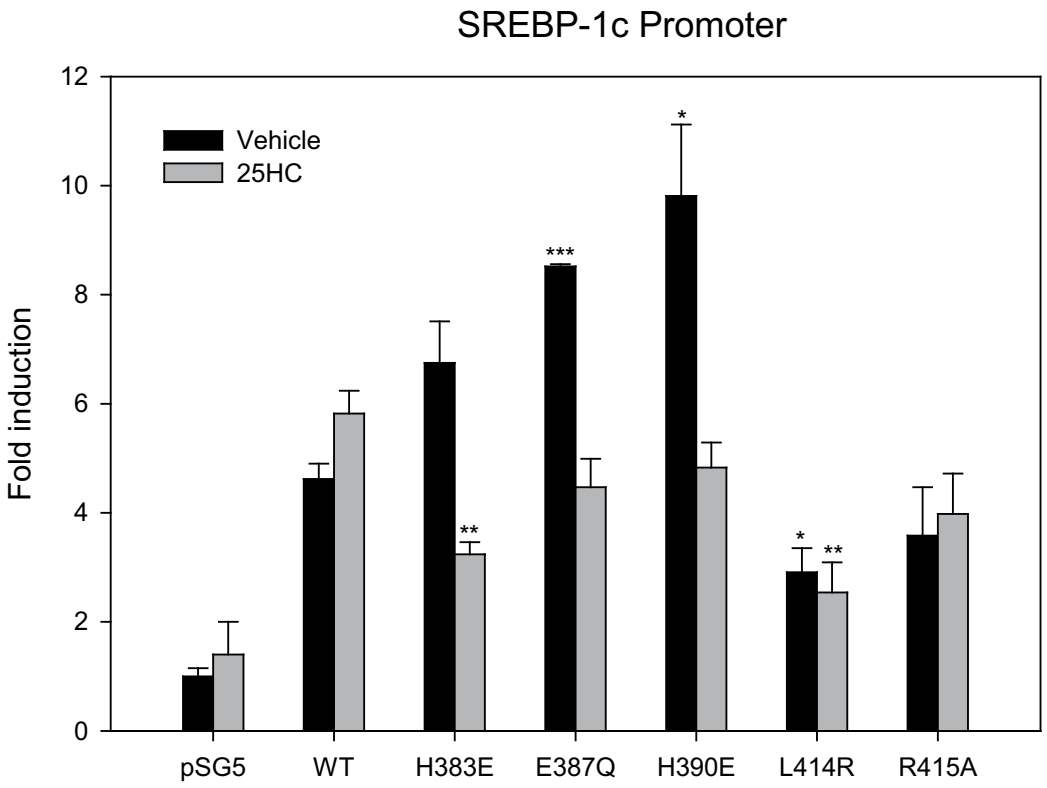

Figure 7: Effect of LXRα interface mutations on luciferase reporter activation of human SREBP-1c promoter. COS-7 cells were co-transfected with pSG5 empty vector or each indicated LXRα plasmid and transactivation of the SREBP-1c LXRE-luciferase reporter construct in the presence of vehicle (solid bars) and 25-HC (Gray bars) was measured. Luciferase reporter activity was measured 18 hrs after the addition of vehicle or ligand and normalized using *Renilla* as an internal control. Asterisks denote significant differences due to the single point mutations compared to wild-type LXRα for vehicle or 25-HC treated cells: $^{*}p < 0.05$, $^{**}p < 0.01$, $^{***}p < 0.001$.

R415A showed no change in promoter activity with the addition of ligand. The effects on ligand-dependent activation of the promoter were not due to effects on ligand binding as all the mutants bind 25-HC as determined through intrinsic quenching assay (Appendix Figure 1 available online at `http://www.agialpress.com/journals/nurr/2017/101302/`). Collectively, these data demonstrate a reduced ability of LXRα mutants to transactivate SREBP-1c promoter in a ligand dependent manner.

Figure 8 shows the effect of LXRα mutations on the ability of LXRα to transactivate ApoA-1 promoter. Overexpression of each of the mutants H383E, E387Q, and L414R alone exhibited similar basal activity as wild-type LXRα. LXRα H390E exhibited enhanced basal activity, whereas R415A exhibited decreased basal activity compared to wild-type LXRα overexpression. This suggests that R415, but not L414, H383E, E3387, and H390, is critical for basal transactivation activity of ApoA1 promoter. All LXRα mutants tested exhibited decreased ligand-induced activation suggesting that the presence of each of these residues is required for ligand-dependent transactvation function of ApoA1 promoter. Cotransfection of LXRα and PPARα resulted in suppression of ApoA1 promoter activity similar to the effects observed on SREBP-1c promoter (data not shown).

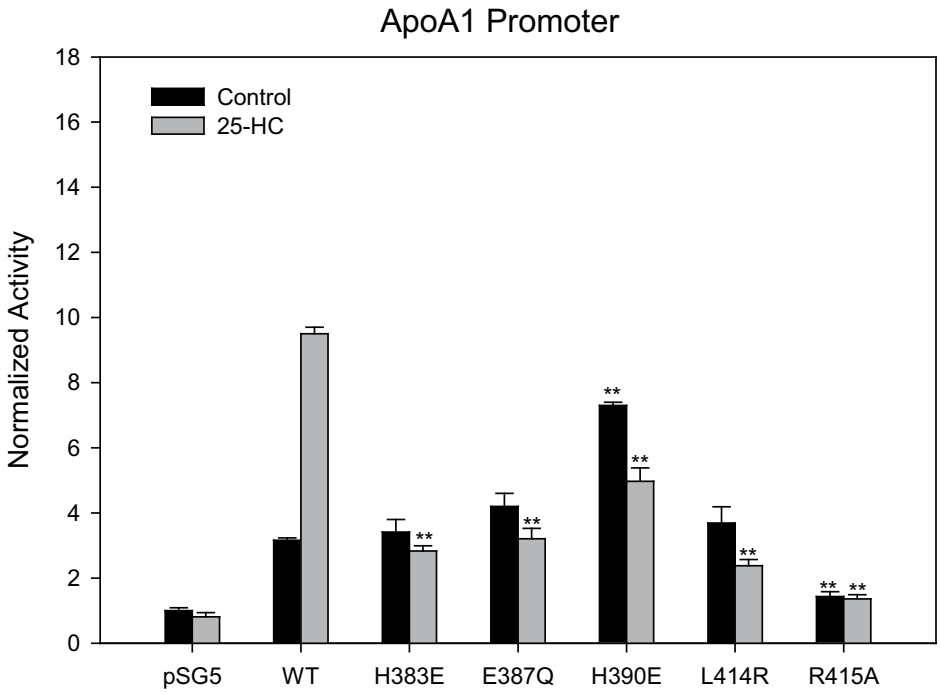

Figure 8: Effect of LXRα interface mutations on luciferase reporter activation of human ApoA1 promoter. COS-7 cells were co-transfected with pSG5 empty vector or each indicated LXRα plasmid and transactivation of the ApoA1 luciferase reporter construct in the presence of vehicle (solid bars) and 25-HC (Gray bars) was measured. Luciferase reporter activity was measured 18 hrs after the addition of vehicle or ligand and normalized using Renilla as an internal control. Asterisks denote significant differences due to the single point mutations compared to wild-type LXRα for vehicle or 25-HC treated cells: $^{*}p < 0.05$, $^{**}p < 0.01$, $^{***}p < 0.001$.

4. Discussion

Sequence alignment coupled with solvent accessibility showed that residues in helices 9 and 10 of LXRα may stabilize the dimer interface to mediate dimerization. Mutants of LXRα were generated through site-directed mutagenesis and evaluated for dimerization through two approaches: (1) *in vitro* protein-protein binding assays, and by (2) bimolecular fluorescence complementation system in living cells. Our results revealed that LXRα L414 is required for the formation of LXRα-RXRα complexes. Consistent with the *in vitro* findings, BiFC analysis showed that mutation of L414 to arginine resulted in disruption of LXRα-RXRα interactions, but not LXRα-PPARα interactions. In the absence of a crystal structure of a LXRα-PPARα complex, it would be interesting to dock the LBDs of individual proteins to determine the nature of interactions at the interface. *In silico* molecular docking showed that R415 forms a hydrogen bond with a serine in RXRβ (1UHL.pdb). However, it is unknown whether LXRα R415 forms a hydrogen bond with PPARα at the same location (glutamine in PPARα).

Complete conservation of LXRα L414 in the corresponding sequences of other NRs suggests that this residue might play a stabilizing role in other RXRα binding proteins. Remarkably, a point mutation in hPPARα (L433R corresponding to L414 in LXRα) abolishes dimerization with RXR [23]. We postulated that substitution of a non-polar, hydrophobic amino acid, L, for the basic amino acid residue R may disrupt an ionic interaction or change the hydrophobic nature of the LXRα interface. As most of the residues involved in the interactions between proteins and

alpha-helices are hydrophobic in nature [24], introducing charge may prove detrimental for the interactions between specific complexes. Moreover, the arrangement of two arginine residues adjacent to each other in L414R mutation may further contribute to destabilization of the dimer. Molecular docking showed that L414R can be accommodated within the dimer core, but without a hydrogen binding partner. The location of this residue is such that it may still be accommodated by changes in the core that impact ligand binding, or by creating a bulge in helix11 that would impact dimerization.

A previous study demonstrated that R415A abolishes ligand dependent transactivation of ADH promoter in response to T-0901317 addition [15]. Our ligand binding result is consistent with the previous observation that R415A does not bind T-0901317. Although the purification properties and the protein yield for the mutants were similar to those observed for wild-type LXRα protein, the altered ligand binding properties of L414R and R415A suggest that changes at the interface might cause subtle rearrangement in the helices lining the LXRα ligand binding pocket. To interpret the mutagenesis data with respect to ligand binding, molecular docking of ligands to the LXRα LBD extracted from the LXRα-RXRβ crystal structure (PDB 1UHL) was performed. The docked models revealed differences in the positioning of T-0901317 in the ligand binding pocket of the energy-minimized mutant receptors. Docking of T-0901317 to the LBDs of LXRα mutants was associated with less favorable binding scores suggesting that interactions mediated by interface residues are crucial for ligand binding. Although the overall conclusion from docking was in agreement with the results obtained from the ligand binding assay, the scoring function did not properly discriminate between conformations of T0901317 in different mutants. For example, LXRα L414R did not bind T0901317 as determined through the quenching of aromatic amino acids, and yet yielded a near wild-type binding score *in silico*. The lack of reliable ranking of the final complexes by docking may be attributed to poor flexibility of the receptor that is not permitted to adjust its conformation upon ligand binding. On the other hand, molecular dynamics simulations would present a more sophisticated approach for structural refinement of the docking complexes and to correctly rank mutants based on their ligand binding abilities [25].

To explain the lack of T-0901317 binding to LXR mutants, we propose that LXRα L414R and R415A mutations might result in a misalignment of key residues (H421 and W443) in the ligand binding pocket. LigPlot analysis showed that T-0901317 was positioned centrally within the ligand binding pocket, however, the head group was situated further away from H421 of LXRα mutants L414R and R415A. Residue His421 has been reported to be critical for agonist binding to LXRα [13] and differential positioning of T-0901317 in L414R and R415A relative to wild-type LXRα could explain the inability of this mutant to bind T-0901317.

Our studies revealed that the CD spectrum of each of the purified mutant LXRα proteins was qualitatively similar to the spectra observed with wild-type LXRα protein suggesting that mutations alone did not result in gross conformational changes in the secondary structure of the proteins (data not shown). However, the calculated and the observed spectra of mixture of PPARα with either L414R or R415A were indistinguishable suggesting no conformational changes occurring in the proteins due to protein-protein binding. Subtle differences were observed between the calculated and the observed CD spectra for H383E, E387Q, and H390E LXRα in the presence of PPARα suggesting that binding of these proteins is accompanied by conformational changes in the dimer structure. It can be concluded that PPARα binding to

LXRα H383E, E387Q, H390E, but not L414R and R415A, resulted in conformational changes in the secondary structure of the dimers.

The effect of mutations on the ability of LXRα to transactivate two promoters: SREBP-1c and ApoA1was examined. The data demonstrated that residues H383, E387, and H390 were not necessary for basal activity of unliganded LXRα, but were required for its ligand-dependent transactivation function. Replacement of L414 with arginine significantly reduced SREBP-1c promoter reporter activity in a ligand dependent as well as ligand independent fashion without affecting the nuclear localization of LXRα. We next investigated whether the effect of L414R mutation on transactivation is promoter specific. The basal transactivation activity of L414R was indeed similar to that of wild-type LXRα on the ApoA1 promoter. However, the ligand dependent transactivation activity on the promoter was abolished. These findings suggest that LXRα mutants (identified here and possibly others that are implicated in metabolic disorders) behave differently depending upon the nature of: (a) mutation, (b) ligand tested, and (c) the promoter under consideration. Thus, a nonresponsive mutant may respond to an alternative ligand to regulate a different subset of genes. The observation that L414R has a lower transactivation activity when challenged with the ligand on SREBP-1c promoter but retains normal wild-type like activity on ApoA1 promoter could have therapeutic implications. Since ApoA1 is the protein component of high density lipoproteins and mediates efflux of cholesterol from the macrophages, L414R presents a possible solution for dissociating the favorable effects of LXRα stimulation from their unwanted effects. For instance, it would be desirable to design a molecule that mimics the effects of L414R mutation such that it exhibits modest SREBP-1c activity (to prevent hypertriglyceridemia) whilst up-regulating transcription of beneficial genes such as ApoA1 (to enhance reverse cholesterol transport).

The phenocopy phenomenon has been used for drug discovery processes through inhibiting a drug target with different functional modulation technologies and thereby mimicking a phenotype of interest [26, 27]. The term phenocopy was introduced by Goldschmidt to describe environmentally induced developmental defects which resemble mutant phenotypes [27, 28]. Inhibition can be achieved using RNA interference (RNAi), to knockdown a target, or by small molecule inhibitors to block or inhibit the activity of the target. Final proof that phenocopy of L414R may offer a solution to the triglyceride-raising problems of the LXRα stimulation must await the identification of molecules that mimic L414R effects in the receptor. Evidence presented herein makes a compelling case for attempting to identify such molecules to develop strategies in combating metabolic disorders.

Competing Interests

The authors declare no competing interests.

Acknowledgement

This work was supported by USPHS NIH grant DK77573 and funds from the Boonshoft School of Medicine and the College of Science and Mathematics, Wright State University.

References

[1] G. A. Francis, E. Fayard, F. Picard, and J. Auwerx, "Nuclear Receptors and the Control of Metabolism," Annual Review of Physiology, vol. 65, pp. 261–311, 2003.

[2] B. A. Janowski, P. J. Willy, T. R. Devi, J. R. Falck, and D. J. Mangelsdorf, "An oxysterol signalling pathway mediated by the nuclear receptor LXRα," Nature, vol. 383, no. 6602, pp. 728–731, 1996.

[3] T. Varga, Z. Czimmerer, and L. Nagy, "PPARs are a unique set of fatty acid regulated transcription factors controlling both lipid metabolism and inflammation," Biochimica et Biophysica Acta, vol. 1812, no. 8, pp. 1007–1022, 2011.

[4] D. J. Peet, S. D. Turley, W. Ma et al., "Cholesterol and bile acid metabolism are impaired in mice lacking the nuclear oxysterol receptor LXRα," Cell, vol. 93, no. 5, pp. 693–704, 1998.

[5] L. Yue, F. Ye, C. Gui et al., "Ligand-binding regulation of LXR/RXR and LXR/PPAR heterodimerizations: SPR technology-based kinetic analysis correlated with molecular dynamics simulation," Protein Science, vol. 14, no. 3, pp. 812–822, 2005.

[6] G. D. Barish, "Peroxisome proliferator-activated receptors and liver X receptors in atherosclerosis and immunity," Journal of Nutrition, vol. 136, no. 3, pp. 690–694, 2006.

[7] J. J. Repa, G. Liang, J. Ou et al., "Regulation of mouse sterol regulatory element-binding protein-1c gene (SREBP-1c) by oxysterol receptors, LXRα and LXRβ," Genes & Development, vol. 14, no. 22, pp. 2819–2830, 2000.

[8] A. Fernández-Alvarez, M. Soledad Alvarez, R. Gonzalez, C. Cucarella, J. Muntané, and M. Casado, "Human SREBF1c expression in liver is directly regulated by peroxisome proliferator-activated receptor α (PPARα)," The Journal of Biological Chemistry, vol. 286, no. 24, pp. 21466–21477, 2011.

[9] D. J. Mangelsdorf, C. Thummel, M. Beato et al., "The nuclear receptor super-family: the second decade," Cell, vol. 83, no. 6, pp. 835–839, 1995.

[10] P. Chambon, "A decade of molecular biology of retinoic acid receptors," The FASEB Journal, vol. 10, no. 9, pp. 940–954, 1996.

[11] H. Gronemeyer and V. Laudet, "Transcription factors 3: nuclear receptors.," Protein profile, vol. 2, no. 11, pp. 1173–1308, 1995.

[12] T. Perlmann and R. M. Evans, "Nuclear receptors in sicily: All in the famiglia," Cell, vol. 90, no. 3, pp. 391–397, 1997.

[13] S. Svensson, T. Ostberg, M. Jacobsson et al., "Crystal structure of the heterodimeric complex of LXRalpha and RXRbeta ligand-binding domains in a fully agonistic conformation," EMBO J, vol. 22, pp. 4625–33, 2003.

[14] S.-K. Lee, B. Lee, and J. W. Lee, "Mutations in retinoid X receptor that impair heterodimerization with specific nuclear hormone receptor," Journal of Biological Chemistry, vol. 275, no. 43, pp. 33522–33526, 2000.

[15] A. I. Shulman, C. Larson, D. J. Mangelsdorf, and R. Ranganathan, "Structural determinants of allosteric ligand activation in RXR heterodimers," Cell, vol. 116, no. 3, pp. 417–429, 2004.

[16] M. Balanarasimha, A. M. Davis, F. L. Soman, S. D. Rider, and H. A. Hostetler, "Ligand-regulated heterodimerization of peroxisome proliferator-activated receptor α with liver X receptor α," Biochemistry, vol. 53, no. 16, pp. 2632–2643, 2014.

[17] D. P. Oswal, M. Balanarasimha, J. K. Loyer et al., "Divergence between human and murine peroxisome proliferator-activated receptor alpha ligand specificities," Journal of Lipid Research, vol. 54, no. 9, pp. 2354–2365, 2013.

[18] D. P. Oswal, G. M. Alter, S. D. Rider Jr., and H. A. Hostetler, "A single amino acid change humanizes long-chain fatty acid binding and activation of mouse peroxisome proliferator-activated receptor α," Journal of Molecular Graphics and Modelling, vol. 51, pp. 27–36, 2014.

[19] N. Sreerama and R. W. Woody, "Estimation of protein secondary structure from circular dichroism spectra: comparison of CONTIN, SELCON, and CDSSTR methods with an expanded reference set," Analytical Biochemistry, vol. 287, no. 2, pp. 252–260, 2000.

[20] C.-D. Hu, Y. Chinenov, and T. K. Kerppola, "Visualization of interactions among bZIP and Rel family proteins in living cells using bimolecular fluorescence complementation," Molecular Cell, vol. 9, no. 4, pp. 789–798, 2002.

[21] H. Greschik, J.-M. Wurtz, P. Hublitz, F. Köhler, D. Moras, and R. Schüle, "Characterization of the DNA-binding and dimerization properties of the nuclear orphan receptor germ cell nuclear factor," Molecular and Cellular Biology, vol. 19, no. 1, pp. 690–703, 1999.

[22] T. Yoshikawa, T. Ide, H. Shimano et al., "Cross-talk between peroxisome proliferator-activated receptor (PPAR) α and liver X receptor (LXR) in nutritional regulation of fatty acid metabolism. I. PPARS suppress sterol regulatory element binding protein-1c promoter through inhibition of LXR signaling," Molecular Endocrinology, vol. 17, no. 7, pp. 1240–1254, 2003.

[23] C. E. Juge-Aubry, A. Gorla-Bajszczak, A. Pernin et al., "Peroxisome proliferator-activated receptor mediates cross-talk with thyroid hormone receptor by competition for retinoid X receptor: possible role of a leucine zipper-like heptad repeat," The Journal of Biological Chemistry, vol. 270, no. 30, pp. 18117–18122, 1995.

[24] I. S. Moreira, P. A. Fernandes, and M. J. Ramos, "Hot spots - A review of the protein-protein interface determinant amino-acid residues," Proteins: Structure, Function and Genetics, vol. 68, no. 4, pp. 803–812, 2007.

[25] H. Alonso, A. A. Bliznyuk, and J. E. Gready, "Combining docking and molecular dynamic simulations in drug design," Medicinal Research Reviews, vol. 26, no. 5, pp. 531–568, 2006.

[26] N. J. Smith and G. Milligan, "Allostery at G protein-coupled receptor homo- and heteromers: Uncharted pharmacological landscapes," Pharmacological Reviews, vol. 62, no. 4, pp. 701–725, 2010.

[27] P. Baum, R. Schmid, C. Ittrich et al., "Phenocopy–a strategy to qualify chemical compounds during hit-to-lead and/or lead optimization.," PloS one, vol. 5, no. 12, Article ID e14272, 2010.

[28] R. Goldschmidt, "Gen und Außeneigenschaft - (Untersuchungen an Drosophila) I," Zeitschrift für Induktive Abstammungs- und Vererbungslehre, vol. 69, no. 1, pp. 38–69, 1935.